PERGAMON

International Journal of Solids and Structures 39 (2002) 959–972

INTERNATIONAL JOURNAL OF SOLIDS and STRUCTURES

www.elsevier.com/locate/ijsolstr

New analytical and numerical results for two-dimensional contact profiles

J. Jäger *

Lauterbach Verfahrenstechnik, Postfach 711 117, D-76338 Eggenstein, Germany

Received 15 January 2001

Abstract

Recently, a generalized Coulomb law for elastic bodies in contact has been developed by the author, which assumes that the tangential traction is the difference of the slip stress of the contact and the stick area, whereby each stick area corresponds to a smaller contact area. It holds for multiple contact regions also. Several applications for elastic half planes, half spaces, thin and thick layers and impact problems have been published. For plane contact of equal bodies with friction, it provides exact solutions, and the interior stress field can be expressed with analytical results in closed form. In this article, a singular superposition of flat punch solutions is outlined, in which the punches are aligned with an edge of the contact area. It is shown that this superposition satisfies Coulomb's inequalities directly, and new results for the Muskhelishvili potentials of several profiles are presented. It is illustrated how problems of singularity and multi-valuedness of complex functions can be solved in closed form, and the Chebyshev approximation used by earlier authors can be avoided. For comparison, some previous solutions for symmetric profiles are appended. Some results for the interior stress field, the pressure, the frictional traction and the surface displacements are compared with FEM solutions of an equivalent problem. The small differences between both methods show characteristic features of the FEM model and the theoretical assumptions, and are shortly explained. Further, this example can be used as benchmark test for FEM and BEM programs.

Keywords: Contact; Elastic friction; Muskhelishvili potential; FEM model; Cattaneo-Mindlin

1. Introduction

Coulomb's law for rigid bodies assumes that if the frictional force be less than a certain amount the bodies do not move. In Contact Mechanics, on the other hand, the bodies are flexible and Coulomb's law is used locally for the stress. When the stress–displacement relations in normal and tangential direction are similar and uncoupled, a normal pressure increment produces the same displacements as a frictional traction increment in tangential direction, and the tangential traction can be written as the difference of the full slip traction of the contact area and the stick area. Each stick area is a smaller contact area or a unique combination of multiple contact areas. The force–displacement relations can be calculated by integration of

* Address: Blattwiesenstr. 7, D-76227 Karlsruhe, Germany. Tel.: +49-9131-64388.
E-mail addresses: www@juergenjaeger.de, j_jaeger@t-online.de (J. Jäger).

0020-7683/02/$ - see front matter
PII: S0020-7683(01)00198-6

the pressure. This result is independent of the mathematical form of the normal contact law on the condition of linear elastic materials in advancing contact (Jäger, 2000). The expression advancing contact means that the whole contact area increases with the force (Gladwell, 1980) and the condition of linear elastic materials allows the superposition of stress distributions. Optional load histories can be written as a superposition of unidirectional displacement increments. This generalized Coulomb model is exact for equal half planes, axisymmetric half spaces and thin layers (Jäger, 1995, 1997a, 1999a). The elastic friction model was also adopted by other researchers (Jäger, 1999b, 2001a). The literature references in this article illustrate the diversity of the method and are not necessary for the understanding of the results. All important equations are listed and a summary of results for different punches is appended at the end.

In this article, the elastic Coulomb law is applied to a flat rounded punch in contact with an elastic plane and compared with FEM results. A FEM analysis of the Hertz contact problem with friction has been published in Chandrasekaran et al. (1987). Recently, several publications appeared on simplified contact laws. A torque–displacement relation for elliptical contact in torsion by Cuttino and Dow (1997) has been discussed by Jäger (1997b). In another paper, it has been suggested to apply simplified force–displacement relations to granular flow simulations by Zhang and Vu-Quoc (2000), and a comparison of tangential force–displacement relations was published by Vu-Quoc and Zhang (1999a). The same authors presented an elastoplastic force–displacement relation with a displacement-driven version in Vu-Quoc and Zhang (1999b) and a force-driven version in Vu-Quoc et al. (2000). More publications can be found in a review on FEM approaches (Mackerle, 1998). The elastic friction law presented in this article cannot be applied to elastic dissimilarity, where the normal and tangential stress–displacement relations are coupled. Contact problems with coupled equations, different contact laws in normal and tangential direction and plastic materials etc, violate the basic assumptions. A simplified model can simulate some typical effects, but it should never be used in the wrong context. It is possible, however, to use the elastic friction law as a general principle for simplified design and parameter studies in machine construction. When some assumptions are violated, worst case scenarios or limiting cases can be used for error estimations. General equations for plates and beams and a survey on solutions for elastic dissimilarity can be found in the book by Gladwell (1980).

The surface displacements u_x and u_z of equal half planes under the surface loading q, p in x- and z-direction, respectively, can be written as integral of point force displacements (Jäger, 1997a)

$$\frac{\pi}{A}\frac{\partial u_x}{\partial x} = -\int_{-a}^{+a} \frac{q(\xi)\,\mathrm{d}\xi}{x-\xi}, \qquad \frac{\pi}{A}\frac{\partial u_z}{\partial x} = -\int_{-a}^{+a} \frac{p(\xi)\,\mathrm{d}\xi}{x-\xi}, \tag{1}$$

$$A = \frac{\kappa_1+1}{4G_1} + \frac{\kappa_2+1}{4G_2}, \qquad \kappa_1 = \begin{cases} 3-4\nu_1, & \text{for plane strain} \\ \frac{3-\nu_1}{1+\nu_1}, & \text{for plane stress} \end{cases} \tag{2}$$

The symbols G_1 and ν_1 denote the shear modulus and Poisson's ratio of body 1, respectively, and the index 2 characterizes values of body 2. The formula for κ_2 can be obtained after substitution of the index 1 with 2 in Eq. (2). It has been explained (Jäger, 1997a) that Eqs. (1) are also exact for a rigid punch in contact with an incompressible elastic half plane (plane strain, $G_2 = \infty$, $\nu_1 = 0.5$).

2. Singular superposition of flat punch solutions

The surface displacements for a singular superposition of flat punches have been presented by Jäger (1998), based on the solution for a flat punch with two square edges at the ends of the contact area at $x = 0$ and a. The pressure $p(a,x)$, the normal displacement $u_z(a,x)$, and the complex Muskhelishvili potential $\phi_p(a,w)$ for a flat punch with two square edges in contact on $0 < x < a$ have the form (Jäger, 1998)

$$p(a,x) = \frac{p_0}{\pi\sqrt{x(a-x)}}, \quad 0 \leqslant x \leqslant a, \tag{3}$$

$$u_z(a,x) = \begin{cases} u_z(a,0), & \text{for } 0 \leqslant x \leqslant a \\ u_z(a,0) - \frac{Ap_0}{\pi} \ln\left(\frac{|2x-a|}{a} + \sqrt{\frac{(2x-a)^2}{a^2} - 1}\right), & x \geqslant a \text{ or } x \leqslant 0 \end{cases} \tag{4}$$

$$\phi_p(a,w) = \frac{\mathrm{i}p_0}{2\pi\sqrt{w(w-a)}}, \quad w = x + \mathrm{i}z, \ \mathrm{i} = \sqrt{-1}. \tag{5}$$

Eq. (4) shows that the displacements are non-singular, in contrast to the point force solution of the integrand in Eq. (1). Therefore, it is possible to avoid the singular integrals, using a superposition of differential flat punches instead of point forces. Several types of superposition are possible, but the resulting integral equations cannot always be solved analytically. Solutions have been published for complete contact, when the punches are aligned with the center of the contact area (Jäger, 1995), and an edge of the contact area (Jäger, 1998). The pressure and the Muskhelishvili potential of the latter have the form

$$p(a,x) = \int_{s=x}^{a} \frac{p_0(s)\,\mathrm{d}s}{\pi\sqrt{x(s-x)}}, \qquad \phi_p(a,w) = \int_{s=0}^{a} \frac{\mathrm{i}p_0(s)\,\mathrm{d}s}{2\pi\sqrt{w(w-s)}}. \tag{6}$$

Eq. (6) shows that the integrand of the pressure has a weak singularity at $x = s$, which can easily be integrated. Further, the pressure has a singularity of the order $x^{-1/2}$ at $x = 0$. The displacement at the point $x \to -0$ of the elastic plane has a vertical slope, which requires a square edge at the origin (Fig. 1). The contact condition for a punch with the profile $z_1(x)$ is illustrated in Fig. 1

$$u_z(a,x)\begin{cases} = u_z(a,0) - z_1(x), & \text{for } x \leqslant a, \quad \text{contact} \\ > u_z(a,0) - z_1(x), & \text{for } x \geqslant a, \quad \text{separation} \end{cases} \tag{7}$$

Superposition of displacements (4) and insertion in Eq. (7) gives an integral equation for the differential forces $p_0(s)$

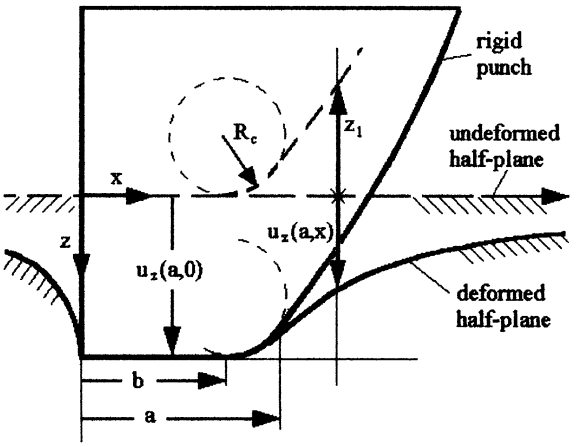

Fig. 1. Flat punch with square edge and rounding.

$$z_1(x) = \frac{A}{\pi}\int_{s=0}^{x} p_0(s)\ln\left(\frac{2x-s}{s} + \sqrt{\frac{(2x-s)^2}{s^2}-1}\right)\mathrm{d}s, \quad 0 \leqslant x \leqslant a. \tag{8}$$

$$\frac{\partial z_1(x)}{\partial x} = \frac{A}{\pi}\int_{s=0}^{x} \frac{p_0(s)\,\mathrm{d}s}{\sqrt{x(x-s)}}, \quad 0 \leqslant x \leqslant a. \tag{9}$$

Eq. (9) is an Abel integral equation and can be inverted

$$p_0(s) = \frac{1}{A}\frac{\partial}{\partial s}\int_{x=0}^{s}\sqrt{\frac{x}{s-x}}\frac{\partial z}{\partial x}\,\mathrm{d}x, \quad 0 \leqslant s \leqslant a. \tag{10}$$

The partial derivative $\partial/\partial s$ in Eqs. (9) and (10) can also be written as absolute derivative $\mathrm{d}/\mathrm{d}s$, because the geometrical and material parameters are constant. The contact condition $p(a,x) > 0$ for the pressure in the contact area holds for the increments $\mathrm{d}p(a,x)$ also, and from Eq. (6) follows $p_0(s) > 0$ as a necessary condition for contact. Eq. (9) on the other hand shows that for the case $0 < p_0(s) < \infty$ the slope must be positive: $\infty > z_1'(x) > 0$ and vice versa. This means that for profiles with a finite slope $z_1'(x) > 0$ the inequality $p(a,x) > 0$ is always satisfied. For $z_1'(x) = 0$, a rigid body motion in form of a flat punch solution can be superposed. Such a general proof cannot be given for the condition of separation (7), which must be checked separately for each profile.

3. Tangential solution

The integral equations in tangential direction (1) are the same as in normal direction and the normal solution can be used for the tangential problem. For simplicity, values of the stick area $x < a^* < a$ will be denoted with asterisk *, e.g. $p^* = p(a^*,x)$, in the equations below. It can easily be shown that the pressure difference $p - p^*$ satisfies the stick condition, which is a constant shift of the stick area (Jäger, 1997a). Thus we obtain the tangential traction q, the force Q and the tangential displacement u_x

$$q = f(p-p^*), \qquad Q = f(P-P^*), \qquad u_x = f\kappa(u_z - u_z^*) \tag{11}$$

with Coulomb's coefficient of friction f. Coulomb's inequality in the stick area

$$q = f(p-p^*) < fp, \text{in the stick area} \tag{12}$$

is always satisfied, because the contact condition for each increment $\mathrm{d}p > 0$ yields $p > p^*$.

The second inequality of Coulomb's law requires that the slip velocity $\mathrm{d}s_t/\mathrm{d}t$ must be opposite to the tangential traction $q = f(p-p^*)$. For constant normal pressure p and decreasing stick areas $\mathrm{d}a^* < 0$, the tangential traction increment $\mathrm{d}q = f\,\mathrm{d}p^* > 0$ at a constant position x depends on the stick radius a^*. The pressure increment $\mathrm{d}q$ is a flat punch solution (Jäger, 1998, Section 2ii). The corresponding slip increment $\mathrm{d}s_t(a^*,x)$ is the difference of the elastic displacement $\mathrm{d}u_x(a^*,x)$ and the rigid body displacement $\mathrm{d}\xi(a^*) = \mathrm{d}u_x(a^*,0)$ of the stick area

$$\mathrm{d}s_t(a^*,x) = \mathrm{d}u_x(a^*,x) - \mathrm{d}u_x(a^*,0) = f\kappa[\mathrm{d}u_z(a^*,x) - \mathrm{d}u_z(a^*,0)], \tag{13}$$

where Eq. (11) was used. Eq. (4) shows that the slip $\mathrm{d}s_t(a^*,x)$ must be negative, and opposite to the traction q, as required by Coulomb's slip inequality. In the case of general load histories, this proof holds also for a superposition of displacement increments. When finite increments are used, as usual in numerical mechanics, it can be shown that Coulomb's inequality is identical with the condition of separation for the normal problem. The differential formulation (13) is more general, and can be used in the same form for

torsion of axisymmetric surfaces (Jäger, 1995). Thus, the validity of Coulomb's inequalities is a direct consequence of the method of superposition of flat rigid punches.

4. Singular flat punch with a rounded edge

In a series of publications (Ciavarella et al., 1998a,b), a Chebyshev expansion has been used for the Muskhelishvili potential of a symmetric flat rounded punch, and a wedge with rounded tip. This potential is useful for the interior stress field, and a simple analytical solution in closed form is derived below. The mentioned publications have been discussed in Jäger (1999b, 2001a). For the special case of a singular flat punch with a rounded edge (Fig. 1), which has a square edge at the origin and a rounding at the other contact end, the gap $z_1(r)$ between the surfaces in undeformed contact has the form

$$z_1(x) = H\left(\frac{x}{b}\right)\frac{(x-b)^2}{2R_c}, \quad \text{for } 0 \leqslant x \leqslant a, \qquad H(x) = \begin{cases} 0, & x < 1 \\ 1, & x \geqslant 1 \end{cases} \tag{14}$$

Insertion of Eq. (14) in Eq. (10) gives

$$2AR_c p_0(s) = H\left(\frac{s}{b}\right)\left\{3\sqrt{b(s-b)} + (3s-2b)\arccos\sqrt{\frac{b}{s}}\right\}. \tag{15}$$

The pressure $p(a,x)$ in Eq. (6) can be evaluated with Eq. (15)

$$\pi AR_c p_1(a,x) = \sqrt{\frac{a-x}{x}}\left[(a+2x-2b)\arccos\sqrt{\frac{b}{a}} + \sqrt{b(a-b)}\right] + (b-x)\ln\frac{\left(\sqrt{b(a-x)} - \sqrt{x(a-b)}\right)^2}{a|b-x|}. \tag{16}$$

The normal force is the integral of differential forces $p_0(s)$

$$P_1(x) = \int_{s=0}^{a} p_0(s)\,\mathrm{d}s = 2AR_c\left\{\sqrt{b(a-b)}\left(\frac{3}{2}a - b\right) + \frac{3}{2}a^2 - 2ba\arccos\sqrt{\frac{b}{a}}\right\} \tag{17}$$

with the coordinates x and z. The Muskhelishvili potential ϕ_{P1} can be calculated by insertion of Eq. (15) in Eq. (6) (Appendix A.1)

$$2\pi AR_c\phi_{p1}(a,w) = \mathrm{i}\sqrt{\frac{w-a}{w}}\left((2b-2w-a)\arccos\sqrt{\frac{b}{a}} - \sqrt{b(a-b)}\right) + 2\mathrm{i}(w-b)\arcsin\sqrt{\frac{w(a-b)}{a(w-b)}}. \tag{18}$$

In Muskhelishvili's definition the z-axis points outside of the body. The derivative $\partial\phi_{P1}/\partial w$ is necessary for the stress calculation

$$4\pi AR_c\frac{\partial\phi_{p1}(a,w)}{\partial w} = \mathrm{i}(2w(a-2w)+a(2b-a))\frac{\arccos\sqrt{b/a}}{\sqrt{w^3(w-a)}} - \mathrm{i}(2w+a)\sqrt{\frac{b(a-b)}{w^3(w-a)}} + 4\mathrm{i}\arcsin\sqrt{\frac{w(a-b)}{a(w-b)}}. \tag{19}$$

The displacement $u_z(a,x)$ follows from Eq. (4), similar as Eq. (8)

$$u_z(a,x) = u_z(a,0) - \frac{A}{\pi}\int_{s=0}^{F} p_0(s)\mathrm{d}s, \qquad F = \min(x,a). \tag{20}$$

Eq. (20) can be integrated numerically. The Muskhelishvili potential for the tangential loading alone has been derived in (Jäger, 1997a)

$$\phi_q(a,a^*,w) = \mathrm{i}f\left(\phi_p(a,w) - \phi_p(a^*,w)\right). \tag{21}$$

The total potential for normal and tangential loading is

$$\phi_{\text{total}}(a,a^*,w) = (1+\mathrm{i}f)\phi_p(a,w) - \mathrm{i}f\phi_p(a^*,w). \tag{22}$$

5. Superposition of punches

The profile z_2 of a wedge with rounded tip (Fig. 2) can be written as the difference of a Hertzian profile and a flat rounded punch z_1 given by Eq. (14)

$$z_2(x) = \frac{x^2}{2R_c} - z_1(x). \tag{23}$$

The profile $z_2(x)$ of the rounded wedge is parabolical for $x < b$ and has a constant slope for $b < x < a$. In linear elasticity, solutions can be superposed linearly, and it is not necessary to calculate a new solution for this case. The Hertzian result is the special case $b = 0$ in Eqs. (14)–(22). As example, the pressure for a wedge with rounded tip in Fig. 2 is the difference of Eq. (16) with $b = 0$ and the same term with $b > 0$.

$$\pi A R_c p_2(a,x) = \sqrt{\frac{a-x}{x}}\frac{\pi}{2}(a+2x) - \pi A R_c p_1(a,x). \tag{24}$$

The solution for a symmetric flat punch with rounded edges (Fig. 3) can be written as symmetric superposition of two singular punches $p_1(a,x) + p_1(a,a-x)$ defined by Eq. (16). A derivation of the solution for the mirrored punch $p_1(a,a-x)$ is outlined in Appendix A.4. This superposition generates symmetric

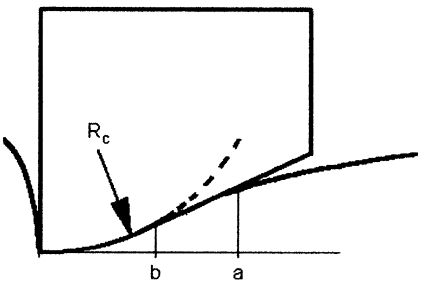

Fig. 2. Rounded wedge.

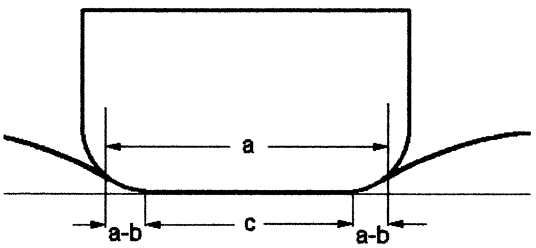

Fig. 3. Flat rounded punch.

singularities at the edges, which can be eliminated by subtraction of a flat punch with two square edges, given by Eq. (3), with

$$p_{03} = \lim_{x\to 0}\{\pi\sqrt{ax}p_1(a,x)\} = a\Big((a-2b)\arccos\sqrt{b/a} + \sqrt{b(a-b)}\Big), \tag{25}$$

$$p_3(a,x) = p_1(a,x) + p_1(a,a-x) - \frac{p_{03}}{\pi A R_c\sqrt{x(a-x)}}, \tag{26}$$

$$\phi_{p3}(a,w) = \phi_{p1}(a,w) - \phi_{p1}(a,a-w) - \frac{\mathrm{i}p_{03}}{2\pi A R_c\sqrt{w(w-a)}}. \tag{27}$$

Numerical comparison shows that Eq. (26) is identical with Schubert's formula (20) and (21) in Schubert (1942). The solutions (26) and (27) for a symmetric flat rounded punch (Fig. 3) have been derived with an alternative symmetric superposition method in Jäger (2001b). A non-symmetric superposition of two punches with the flat regions b_1 and b_2 in Fig. 1 is straightforward, i.e. the limit $\sqrt{x}p_1(a,b_1,x)$ for $x\to 0$ must be identical with the limit $\sqrt{(a-x)}p_1(a,b_2,a-x)$ for $x\to a$. This gives a non-linear equation for b_2 and b_1, as a function of the contact length a, such that a flat punch with two square edges (3) can be subtracted. It is necessary that the punches have complete contact on the whole contact area and that both singularities are equivalent. The resulting punch of this superposition has a flat region of the length $b = b_1 + b_2 - a$, such that the dependent variables b_1 and b_2 can be eliminated for a given contact length a. More profiles are presented in Appendix A.1 and A.2, which can be used for similar superpositions. Consideration of limiting cases and numerical calculations as below can be helpful for the verification of new solutions.

6. Interior stress field

The von Mises stress σ_a can be expressed in terms of the strain energy due to distortion (Jäger, 1997a)

$$\begin{aligned}&\sigma_a^2 = \sigma_x^2+\sigma_y^2+\sigma_z^2-(\sigma_x\sigma_y+\sigma_y\sigma_z+\sigma_x\sigma_z)+3(\tau_{xy}^2+\tau_{yz}^2+\tau_{xz}^2).\\ &\text{Plane stress}: \sigma_y = \tau_{xy} = \tau_{yz} = 0,\\ &\text{Plane strain}: \sigma_y = \nu(\sigma_x+\sigma_z),\quad \tau_{xy} = \tau_{yz} = 0.\end{aligned} \tag{28}$$

The stress components can be written as a function of the Muskhelishvili potential

$$\begin{aligned}&\gamma_1 = \tfrac{1}{2}(\sigma_x+\sigma_z) = \phi(w) + \overline{\phi(w)},\\ &\delta_1 = \tfrac{1}{2}(\sigma_z-\sigma_x+2\mathrm{i}\tau_{xz}) = (\overline{w}-w)\phi'(w) + \overline{\phi(\overline{w})} - \phi(w).\end{aligned} \tag{29}$$

The bar denotes conjugate complex values. Insertion of Eq. (29) in Eq. (28) gives

$$\sigma_a^2 = \begin{cases}\gamma_1^2 + 3\delta_1\overline{\delta_1}, & \text{for plane stress}\\ (1-2\nu)^2\gamma_1^2 + 3\delta_1\overline{\delta_1}, & \text{for plane strain}\end{cases} \tag{30}$$

The complex functions can easily be evaluated with mathematical software packages, and an example for Mathematica has been presented in (Jäger, 1997a).

7. Comparison with FEM

The solutions (26) and (27) for a symmetric flat rounded punch have been compared with a FEM calculation at the conference Contact Mechanics V by Jäger (2001b), and are shortly summarized in this section. Fig. 4 illustrates the FEM model, which was solved with ANSYS 5.5. Rigid elements TARGE169

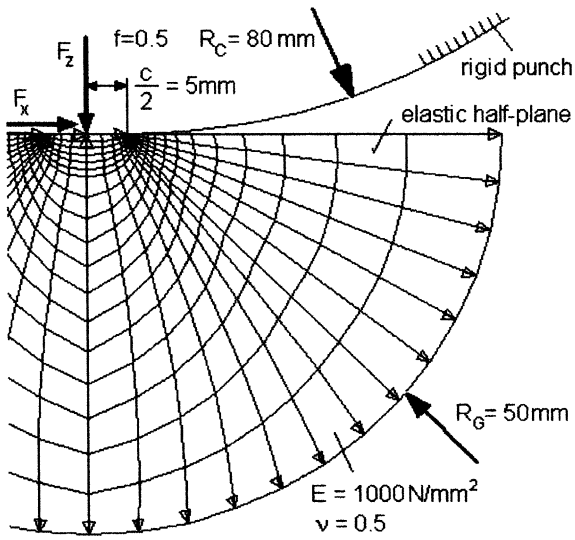

Fig. 4. FEM mesh.

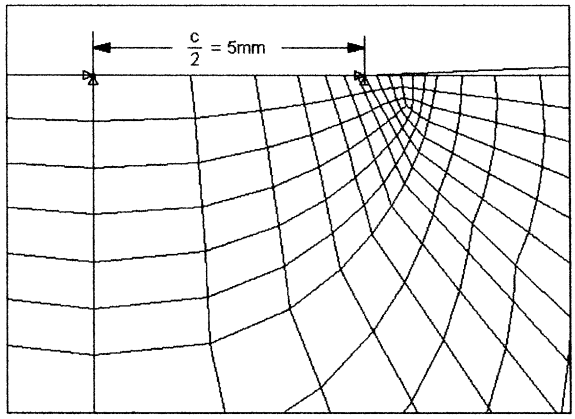

Fig. 5. Model of the contact region.

are used to represent the rigid punch with the semi-axis $c/2 = 5$ mm of the flat region and the rounding radius $R_c = 80$ mm. A circular region of the half plane is modeled with 2-D elements PLANE42 and is fixed radially at $R_G = 50$ mm. The x-axis of the half plane represents the contact surface and consists of CONTA171 elements, which are associated with the target elements. The half plane has a modulus of Elasticity $E = 1000$ N/mm^2, Poisson's ratio $v = 0.4999 \approx 0.5$ and a coefficient of friction $f = 0.5$. The normal force is applied in steps 1–3, calculated as superposition of Eq. (17) for the semi-axes $a/2 = \{5.4, 5.8, 6.2\}$ of the contact area. Four increments are used for each step. After normal loading, a tangential force is applied in steps 4–6, with the values $a^*/2 = \{5.8, 5.4, 0\}$ for the semi-axis of the stick area. With these values, the normal solution can directly be inserted in Eqs. (11) for the tangential problem, e.g. as the traction: $q = f(p(a,x) - p(a^*,x))$ (Fig. 5).

A comparison between the normal pressure of ANSYS (markers) and the analytical result (full line) is shown in Fig. 6. The difference between both methods is very small. The vertical slope of the pressure

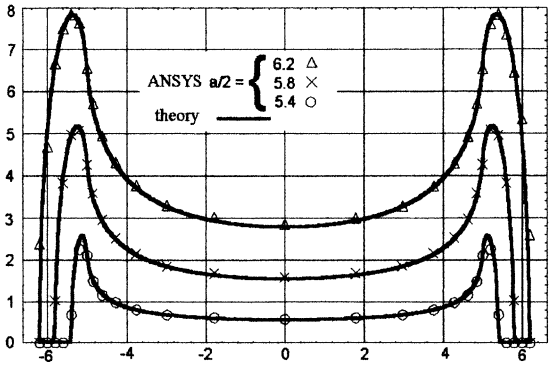

Fig. 6. Pressure for steps 1–3.

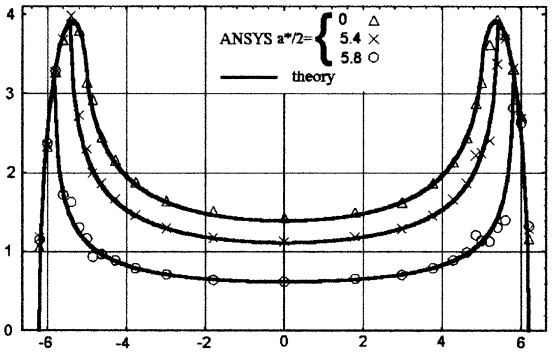

Fig. 7. Surface traction for steps 4–6.

$\partial p(a,x)/\partial x = \infty$ at the positions $x = a/2$ and $x = c/2$ is very typical for a discontinuous variation of the curvature. The difference between the theoretical and numerical tractions of steps 4–6 in Fig. 7 is larger. Small oscillations are visible in the diagram, which depend on the discretization of the FEM mesh, and may be a consequence of the Lagrange method. Another difference is a small asymmetry in the traction, which results from the shift of the stick area. This is clearly visible for the frictional traction marked with crosses for $a^*/2 = 5.4$, where the tip of the traction is larger on the left side. The reason of this discrepancy is the analytical assumption of an undeformed contact surface, which neglects the geometrical non-linearity produced by the moving stick zone.

The interior stress field of the numerical (Fig. 8) and analytical solution (Fig. 9) is illustrated for step 5 in the regime of partial slip ($a^*/2 = 5.4$). The maximum and the form of the contours are the same for both methods, but the discrete FEM mesh produces some corners in the contours. The interior stress field differs characteristically from the classical Hertz solution, because the stress concentrations appear at the discontinuities of the curvature. This effect is important for non-Hertzian surfaces with discontinuous curvatures.

Finally, the numerical (markers) and analytical (full line) tangential surface displacements are compared in Fig. 10. The tangential displacement was fixed at the end of the x-axis $x = R_G = 50$ mm. It can be seen that the displacements agree very well.

It may be concluded that for small displacements the FEM model agrees very well with the theory, as long as the geometrical and material non-linearities can be neglected.

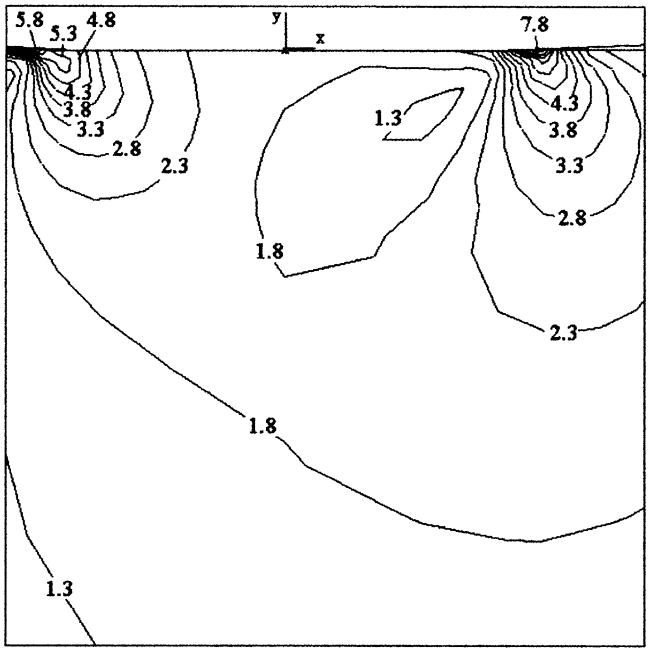

Fig. 8. Ansys solution for step 5.

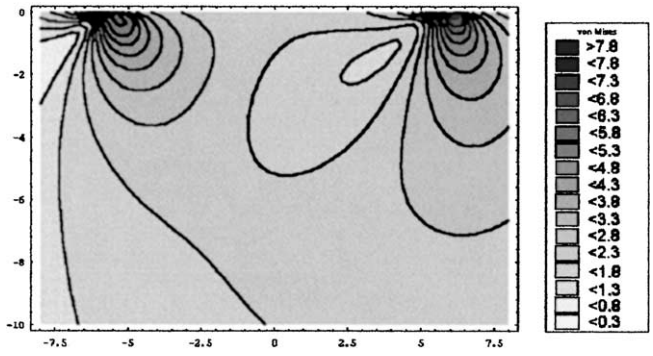

Fig. 9. Analytical solution for step 5.

Appendix A

A.1. Muskhelishvili potential for a singular flat punch with rounding

The arccos term in Eqs. (5) and (15) can be eliminated using integration by parts.

$$4\pi AR_c\sqrt{w}\phi_p(a,w) = 2\mathrm{i}\sqrt{w-a}(2b-2w-a)\arccos\sqrt{\frac{b}{a}} + \mathrm{i}\sqrt{b}\int_{s=b}^{a}\frac{2s^2 - s(b+w) + 2w(w-b)}{s\sqrt{(s-b)(w-s)}}\,\mathrm{d}s \tag{A.1}$$

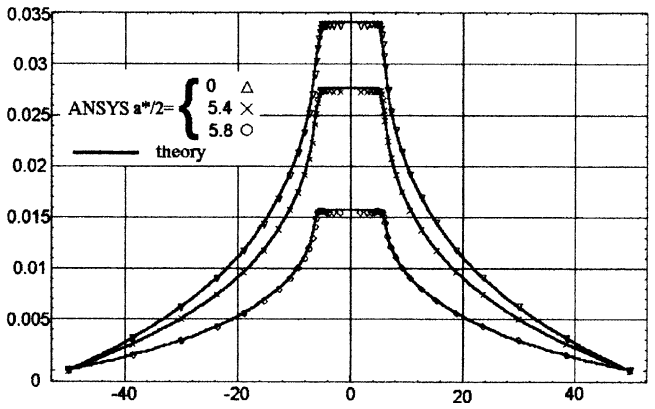

Fig. 10. Surface displacements u_x.

The first two terms of the integrand (A.1) are

$$\mathrm{i}\sqrt{b}\int_{s=b}^{a}\frac{2s^2-s(b+w)}{s\sqrt{(s-b)(w-s)}}\,\mathrm{d}s=-2\mathrm{i}\sqrt{b(a-b)(w-a)}. \tag{A.2}$$

The following substitution of the last term of the integrand gives Eq. (18)

$$z=\sqrt{\frac{a(s-b)}{s(a-b)}}. \tag{A.3}$$

A.2. Polynomial punch with a singular edge

We shortly summarize the solution for a polynomial profile with a singular edge (Jäger, 1998), and include a new formula for the Muskhelishvili potential (Fig. 11)

$$z(x)=A_\alpha x^\alpha, \tag{A.4}$$

$$p_0(s)=\frac{\sqrt{\pi}\alpha A_\alpha\Gamma(\alpha+0.5)}{A\Gamma(\alpha)}s^{\alpha-1}, \tag{A.5}$$

$$P(a)=\frac{\sqrt{\pi}\Gamma(\alpha+0.5)}{A\Gamma(\alpha)}z(a), \tag{A.6}$$

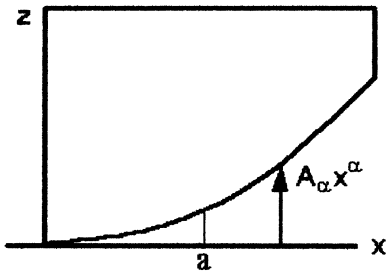

Fig. 11. Polynomial punch with edge.

$$p(a,x) = P(a)\frac{2\alpha}{\pi a}\sqrt{\frac{a-x}{x}}F\left(1,1-\alpha;\frac{3}{2};\frac{a-x}{x}\right), \quad 0 \leqslant x \leqslant a. \tag{A.7}$$

$$\phi_p(a,w) = \frac{\mathrm{i}P(a)}{2\pi w}F\left(\alpha,\frac{1}{2};\alpha+1;\frac{a}{w}\right). \tag{A.8}$$

$$\frac{\partial\phi_p(a,w)}{\partial w} = \frac{-\mathrm{i}P(a)}{2\pi w^2}F\left(\alpha,\frac{1}{2};\alpha+1;\frac{a}{w}\right) + \frac{\mathrm{i}aP(a)\alpha}{4\pi w^3(\alpha+1)}F\left(\alpha+1,\frac{3}{2};\alpha+2;\frac{a}{w}\right). \tag{A.9}$$

A.3. Symmetric polynomial punch

The solution for a symmetric polynomial punch (Jäger, 1995) is summarized for comparison.

$$z(x) = A_\alpha x^\alpha, \tag{A.10}$$

$$p_0(s) = \frac{\alpha P(a)}{a^\alpha}s^{\alpha-1}, \tag{A.11}$$

$$P(a) = \frac{2\sqrt{\pi}\Gamma((\alpha+1)/2)}{A\Gamma(\alpha/2)}z(a), \tag{A.12}$$

$$p(a,x) = P(a)\frac{\alpha}{\pi a}\sqrt{1-\frac{x^2}{a^2}}F\left(1,\frac{2-\alpha}{2};\frac{3}{2};1-\frac{x^2}{a^2}\right), \quad 0 \leqslant x \leqslant a. \tag{A.13}$$

$$\phi_p(a,w) = \frac{\mathrm{i}P(a)}{2\pi w}F\left(\frac{\alpha}{2},\frac{1}{2};\frac{\alpha+2}{2};\frac{a^2}{w^2}\right). \tag{A.14}$$

$$\frac{\partial\phi_p(a,w)}{\partial w} = \frac{-\mathrm{i}P(a)}{2\pi w^2}F\left(\frac{\alpha}{2},\frac{3}{2};\frac{\alpha+2}{2};\frac{a^2}{w^2}\right). \tag{A.15}$$

The Muskhelishvili potential for a symmetric wedge with a sharp edge ($\alpha = 1$ in Fig. 12) has the form (Jäger 1995)

$$\phi_p(a,w) = \frac{\mathrm{i}P(a)}{2\pi a}\arcsin\left(\frac{a}{w}\right), \qquad \frac{\partial\phi_p(a,w)}{\partial w} = \frac{-\mathrm{i}P(a)}{2\pi w\sqrt{w^2-a^2}}. \tag{A.16}$$

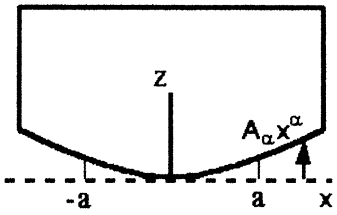

Fig. 12. Symmetric punch.

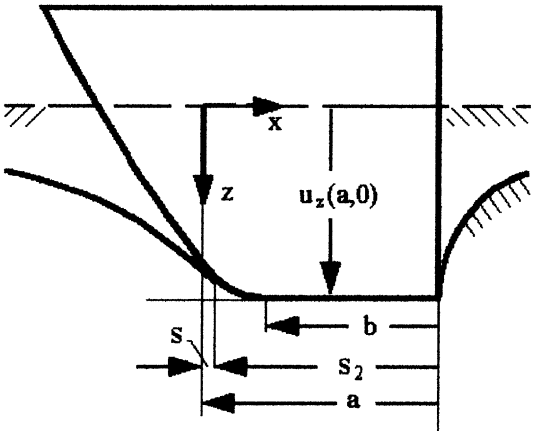

Fig. 13. Reflected flat rounded punch.

A.4. Mirrored flat punch with rounding and singularity

The solution for a flat punch in contact on $s < x < a$ follows from Eqs. (3)–(5) after substitution of (Fig. 13)

$$x_{\text{new}} = x + s_{\text{new}}, \qquad a_{\text{new}} = a + s_{\text{new}}. \tag{A.17}$$

Insertion of Eq. (A.17) in Eq. (4) and omission of the index *new* gives the displacement outside of the contact area

$$u_{z2}(a,x) = u_{z2}(a,a) - \frac{A}{\pi} p_{02}(s) \ln\left(\frac{|2x - s - a|}{a - s} + \sqrt{\frac{(2x - s - a)^2}{(a - s)^2} - 1} \right), \quad x \leqslant s \text{ or } x \geqslant a. \tag{A.18}$$

The flat punch solutions can be superposed analogously to Section 2. The gap z_2 must be the integral of the displacement increments before the point x makes contact

$$z_2(a,x) = \frac{A}{\pi} \int_{s=x}^{a} p_{02}(s) \ln\left(\frac{a + s - 2x}{a - s} + \sqrt{\frac{(a + s - 2x)^2}{(a - s)^2} - 1} \right), \quad 0 \leqslant x \leqslant a. \tag{A.19}$$

$$\frac{\partial z_2(x)}{\partial x} = -\frac{A}{\pi} \int_{s=x}^{a} \frac{p_{02}(s)\,\mathrm{d}s}{\sqrt{(s - x)(a - x)}}, \quad 0 \leqslant x \leqslant a. \tag{A.20}$$

Substitution of

$$s = a - s_2, \qquad x = a - x_2 \tag{A.21}$$

gives

$$\frac{\partial z_2(x)}{\partial x_2} = \frac{A}{\pi} \int_{s_2=0}^{x_2} \frac{p_{02}(s_2)\,\mathrm{d}s_2}{\sqrt{(x_2 - s_2)x_2}}. \tag{A.22}$$

Comparison with Eq. (9) shows

$$p_{02}(s) = p_{01}(a - s), \tag{A.23}$$

where the index 1 denotes the solution for the corresponding reflected punch of Section 4. We perform the same operation for the pressure

$$p_{z2}(a,x) = \int_{s=0}^{x} \frac{p_{02}(s)\,\mathrm{d}s}{\pi\sqrt{(x-s)(a-x)}} = \int_{s_2=x_2}^{a} \frac{p_{01}(s_2)\,\mathrm{d}s_2}{\pi\sqrt{x_2(s_2-x_2)}} = p_{z1}(a,a-x). \tag{A.24}$$

The Muskhelishvili potential

$$\phi_{p2}(a,w) = \int_{s=0}^{a} \frac{\mathrm{i}p_{02}(s)\,\mathrm{d}s}{2\pi\sqrt{(w-s)(w-a)}} \tag{A.25}$$

can be reformulated in the same way as Eq. (A.24), with $w_2 = a - w$

$$\phi_{p2}(a,w) = \int_{s=0}^{a-b} \frac{-\mathrm{i}p_{02}(s)\,\mathrm{d}s}{2\pi\sqrt{(s-w)(a-w)}} = \int_{s_2=b}^{a} \frac{-\mathrm{i}p_{01}(s_2)\,\mathrm{d}s_2}{2\pi\sqrt{w_2(w_2-s_2)}}, \quad w_2 = a - w. \tag{A.26}$$

The result is

$$\phi_{p2}(a,w) = -\phi_{p1}(a,a-w) \tag{A.27}$$

with ϕ_{p1} defined by Eq. (18).

References

Chandrasekaran, H., Haisler, W.E., Goforth, R.E., 1987. Finite element analysis of Hertz contact problem with friction. Finite Elements Anal. Des. 3, 39–56.

Ciavarella, M., Hills, D.A., Monno, G., 1998a. The influence of rounded edges on indentation by a flat punch. ImechE, Proc. Instn. Mech. Engrs. 212 (part C), 319–328.

Ciavarella, M., Hills, D.A., Monno, G., 1998b. Contact problems for a wedge with rounded apex. Int. J. Mech. Sci. 40, 977–988.

Cuttino, J.F., Dow, T.A., 1997. Contact between elastic bodies with an elliptic contact interface in torsion. J. Appl. Mech. 64, 144–148.

Gladwell, G.M.L., 1980. Contact problems in the classical theory of elasticity. Sijthoff & Noordhoff, Alphen aan den Rijn, The Netherlands.

Jäger, J., 1995. Axi-symmetric bodies of equal material in contact under torsion or shift. Arch. Appl. Mech. 65, 478–487.

Jäger, J., 1997a. Half-planes without coupling under contact loading. Arch. Appl. Mech. 67, 247–259.

Jäger, J., 1997b. Discussion of Contact between elastic bodies with an elliptic contact interface in torsion by Cuttino & Dow. J. Appl. Mech. 64, 1022–1024.

Jäger, J., 1998. A new principle in contact mechanics. J. Tribology 120, 677–685.

Jäger, J., 1999a. Equal layers in contact with friction. In: Gaul L., Brebbia, C.A., (Eds.), Contact mechanics IV. Wessex Institute of Technology, WIT Press, pp. 99–108.

Jäger, J., 1999b. Discussion of Tangential loading of general three-dimensional contact. J. Appl. Mech. 66, 1048–1049.

Jäger, J., 2000. Conditions for the generalization of Cattaneo-Mindlin, Presentation at the GAMM-meeting 1999. Z. angew. Math. Mech. 80, S383–S384.

Jäger, J., 2001a. Some comments on recent generalizations of Cattaneo-Mindlin. Int. J. Solids Struct. 38 (14), 2453–2459.

Jäger, J., 2001b. New analytical solutions for a flat rounded punch compared with FEM. In: Domínguez, J., Brebbia, C.A., (Eds.), Contact mechanics V. Wessex Institute of Technology, WIT-press, pp. 307–316.

Mackerle, J., 1998. Contact mechanics—Finite element and boundary element approaches—A bibliography (1995–1997). Finite Elements Anal. Des. 29, 275–285.

Schubert, G., 1942. Zur Frage der Druckverteilung unter elastisch gelagerten Tragwerken. Ing. Arch. 13, 132–147.

Vu-Quoc, L., Zhang, X., 1999a. An accurate and efficient tangential force–displacement model for elastic frictional contact in particle-flow simulations. Mech. Mater. 31, 235–269.

Vu-Quoc, L., Zhang, X., 1999b. An elasto-plastic contact force–displacement model in the normal direction: Displacement-driven version. Proc. R. Soc. Lond. A 455, pp. 4013–4044.

Vu-Quoc, L., Zhang, X., Lesburg, L.A., 2000. A normal force–displacement model for contacting spheres accounting for plastic deformation: Force-driven formulation. J. Appl. Mech. 67, 363–371.

Zhang, X., Vu-Quoc, L., 2000. Simulation of chute flow of soybeans using and improved tangential force–displacement model. Mech. Mater. 32, 115–129.